

Electronic Supplementary Information for

Efficient electrocoupling of CO₂ and N₂ to urea by a gas-penetrable Bi nanosheet-wrapped Cu hollow fiber

Jinning Wang,^{a,b,c} Yuyu Wang,^d Fang Wang,^{*a,b,c} Jinfu Ma,^e Zhengguo Zhang,^{a,b,c} and
Shixiong Min^{*a,b,c,d}

^a School of Chemistry and Chemical Engineering, North Minzu University, Yinchuan, 750021, P. R. China. E-mail: sxmin@nun.edu.cn; wangfang987@126.com

^b Ningxia Key Laboratory of Solar Chemical Conversion Technology, North Minzu University, Yinchuan 750021, P. R. China.

^c Key Laboratory of Chemical Engineering and Technology, State Ethnic Affairs Commission, North Minzu University, Yinchuan, 750021, P. R. China.

^d Analysis and Testing Center of Ningxia Hui Autonomous Region, North Minzu University, Yinchuan, 750021, P. R. China.

^e School of Materials Science and Engineering, North Minzu University, Yinchuan 750021, P. R. China.

1. Experimental

1.1 Chemicals and materials

All chemicals were used as received without further purification. Cu powder (99.9%, 1 μm) was purchased from Zhongmai Metal Materials Co., Ltd. Polyetherimide (PEI, molecular weight: 628.62 Da) was purchased from Saudi Basic Industries Corporation (SABIC). Diacetyl monoxime ($\text{C}_4\text{H}_7\text{NO}_2$, $\geq 98\%$), N-methyl-2-pyrrolidone (NMP, $\geq 99.0\%$), and potassium bicarbonate (KHCO_3 , $\geq 99.5\%$) were purchased from Shanghai Titan Scientific Co., Ltd. Bismuth chloride (BiCl_3 , $\geq 98\%$), thiosemicarbazone ($\text{CH}_3\text{N}_3\text{S}$, $\geq 99.0\%$), concentrated sulfuric acid (H_2SO_4 , $\geq 98\%$), and concentrated hydrochloric acid (HCl , 36~38%) were purchased from Sinopharm Chemical Reagent Co., Ltd. Dimethyl sulfoxide (DMSO, $\geq 99.5\%$), phosphoric acid (H_3PO_4 , 98%), and anhydrous ethanol ($\text{C}_2\text{H}_5\text{OH}$, $\geq 99.7\%$) were purchased from Tianjin Damao Co., Ltd. Ferric chloride ($\text{FeCl}_3 \cdot 6\text{H}_2\text{O}$, $\geq 99.0\%$) and urea (H_2NCONH_2 , $\geq 99.0\%$) were purchased from Tianjin Dingxin Chemical Industry Co., Ltd. The high-purity carbon dioxide (CO_2 , 99.999%), nitrogen (N_2 , 99.999%), and argon (Ar, 99.999%) were purchased from Jinghua Industrial Gas Co., Ltd. Nafion 117 membrane was purchased from by Alfa Aesar Chemical Co., Ltd. Ultrapure water (18.2 $\text{M}\Omega \text{ cm}$) was obtained from a water purification system (Hitech ECO-S15).

1.2 Electrodes preparation

1.2.1 Fabrication of Cu hollow fiber (Cu HF)

Cu HF was fabricated according to a previously reported phase-inversion/sintering process.¹ In brief, 5 g of PEI powder was first added into 15 g of NMP solution followed by heating treatment at 80 $^\circ\text{C}$ for 8 h to obtain a transparent solution, to which 30 g of Cu powder was added. The as-obtained mixture was then subjected to ball milling (300 rpm) for 3 h to form a homogeneous slurry. After cooling to room temperature, the

slurry was vacuumized (1 mbar) for 12 h to remove the bubbles and obtain a casting solution. Next, the casting solution was extruded through a spinning machine and shaped in a water bath *via* the phase-inversion process. After spinning, the as-formed tubes were kept in a water bath for 24 h to eliminate the NMP followed by stretching and drying for 48 h to obtain a Cu HF precursor. The Cu HF precursor was cut into 6 cm in length and then calcinated at 600 °C with a ramping rate of 1 °C·min⁻¹ for 6 h in an air flow (150 mL·min⁻¹) to remove PEI. After being naturally cooled to room temperature, the calcined Cu HF precursor was then reduced at 500 °C (heating rate: 1 °C·min⁻¹) for 3 h in a 10% H₂ (argon balanced) flow (100 mL·min⁻¹) to obtain Cu HF.

1.2.2 Fabrication of Bi NSAs@Cu HF electrode

The Bi NSAs@Cu HF electrode was fabricated *via* the well-established galvanic replacement reaction (GRR).² The Cu HF was first washed with diluted HCl (1 M) for 10 min to remove the native oxide layer, then washed with deionized water and ethanol in turn, and finally dried in a N₂ flow at room temperature. Afterward, the clean Cu HF (2.5 cm) was immersed in 40 mL of DMSO solution containing BiCl₃ (20 μM) for 3h. The obtained Bi NSAs@Cu HF electrode was rinsed with ethanol several times and dried under N₂ flow at room temperature.

1.3 Characterizations

X-ray diffraction (XRD) patterns were analyzed in the 2θ range of 5~80° with a scanning rate of 5° min⁻¹ using a Rigaku Smartlab diffractometer with Cu $K\alpha$ radiation, operating at 40 kV and 40 mA. Scanning electron microscopy (SEM) images and energy X-ray spectrometer (EDX) were taken with a SIGMA 500 scanning electron microscope. Transmission electron microscopy (TEM) images were taken with a FEI Talos F200x field emission transmission electron microscope. X-ray photoelectron spectroscopy (XPS) measurements of the samples were performed on a Thermo Fisher

Escalab-250Xi electron spectrometer using an Al K α X-ray source. All spectra were calibrated according to the C 1s binding energy at 284.8 eV. The atomic force microscopy (AFM) images were taken with Bruker Dimension Icon atomic force microscopy, and the scanning range was 2 \times 2 μ m.

1.4 Gas permeability measurements

The gas permeability of the electrodes was measured with a custom gas permeability device.³ The gas permeability of the HF electrodes was calculated by measuring gas flux and pressure drop across the HF electrode using the following equation:

$$P = F / (A \times \Delta p)$$

where P is the gas permeability ($\text{mol m m}^{-2} \text{pa}^{-1} \text{s}^{-1}$), F is the molar flow rate (mol s^{-1}), A is the HF's outer surface area (m^2), and Δp is the pressure drop (pa) across the HF. P was reported in unit of GPU (1 GPU= $3.35 \times 10^{-10} \text{ mol m m}^{-2} \text{pa}^{-1} \text{s}^{-1}$).

1.5 Electrocatalytic coreduction of CO₂ and N₂ in the H-type cell

All the electrochemical experiments were conducted in an H-type electrochemical cell separated by a Nafion 117 membrane with a potentiostat (CS350M; Corrtest Instruments). A Pt mesh and a saturated Ag/AgCl electrode were used as the counter electrode and reference electrode, respectively. A 0.1 M KHCO₃ solution was used as the supporting electrolyte. The gas-penetrable working electrode was assembled by sticking HF tube (Cu HF or Bi NSAs@Cu HF) into a Cu tube using conductive silver adhesive, while the end of the HF tube as well as the joints between the HF tube and Cu tube were sealed with nonconductive epoxy. The Cu tube was then connected to one inlet for gas flow in at a total rate of 30 mL min⁻¹ (N₂: 15 mL min⁻¹; CO₂:15 mL min⁻¹). Before carrying out all the electrochemical measurements, the 0.1 M KHCO₃ electrolyte solution was purged with CO₂ and N₂ for 30 min. All potentials were measured against a saturated Ag/AgCl electrode reference electrode and converted to

the RHE reference using $E \text{ (vs. RHE)} = E \text{ (vs. Ag/AgCl)} + 0.0591 \times \text{pH} + 0.197$. Linear sweep voltammetry (LSV) measurements were carried out in N_2 - and CO_2 -saturated 0.1 M KHCO_3 solution at a scan rate of 10 mV s^{-1} . Electrical double-layer capacitances of the electrodes were determined by performing cyclic voltammetry (CV) measurements in a non-Faradaic region (0.38~0.48 V) in an Ar-purged 0.1 M KHCO_3 solution. The electrochemical impedance spectroscopy (EIS) measurements were performed in a frequency range from 0.01 Hz to 100 kHz at a voltage amplitude of 5 mV.

1.6 Determination of urea concentration by diacetyl monoxime method

The urea concentration was determined by the diacetyl monoxime method.⁴ 10 mL concentrated phosphoric acid was mixed with 30 mL of concentrated sulfuric acid and 60 mL ultrapure water, then 10 mg FeCl_3 was dissolved in the above solution, denoted as the acid-ferric solution. Then, 0.5 g of diacetyl monoxime (DAMO) and 10 mg of thiosemicarbazone (TSC) were dissolved in ultrapure water and diluted to 100 mL, denoted as DAMO-TSC solution. Typically, 1 mL of the sample solution was removed from the cathodic chamber. Afterward, 1 mL of DAMO-TSC solution and 2 mL of acid-ferric solution was added into 1 mL of sample solution. Next, the mixed solution was heated to $100 \text{ }^\circ\text{C}$ and maintained at this temperature for 15 min. When the solution cooled to $25 \text{ }^\circ\text{C}$, the UV-Vis absorption spectrum was collected at a wavelength of 525 nm. The concentration-absorbance curve was calibrated using standard urea solution for a series of concentrations. The fitting curve shows good linear relation of absorbance value with urea concentration by three times independent calibration tests.

1.7 Calculation of Faradaic efficiency (FE) and urea yield

The urea production was further assessed by performing constant potential electrolysis at the potentials ranging from -0.1 V to -0.5 V vs. RHE . The cathodic liquid products were collected at the end of each electrolysis, and a quantitative analysis was

conducted. The FE for urea electrosynthesis was defined as the amount of electric charge used for producing urea divided by the total charge passed through the electrodes during the electrolysis. Assuming six electrons were needed to produce one urea molecule, the FE was calculated according to the following equation:

$$FE = 6 \times F \times C_{urea} \times V / (60.06 \times Q)$$

The rate of formation of urea was calculated using the following equation:

$$Urea\ yield = C_{urea} \times V / S \times t$$

where F is Faraday constant ($96485\ C\ mol^{-1}$), C_{urea} is the measured mass concentration of urea, V is the volume of the cathodic reaction electrolyte, Q is the electric quantity of charge passing through, t is the time for which the potential was applied, S is the electrode area entering the electrolyte.

2. Additional data

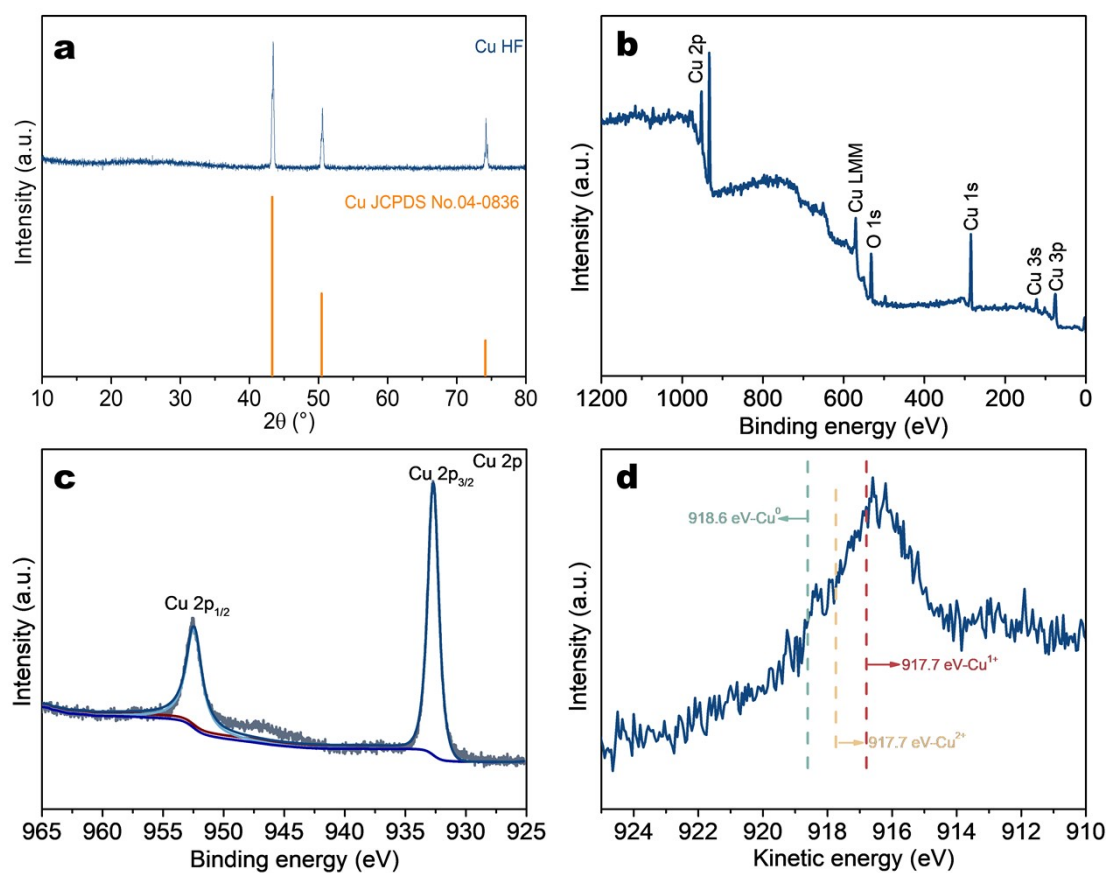


Fig. S1 (a) XRD pattern of Cu HF. (b) Survey, (c) Cu 2p, and (d) Cu LMM Auger XPS spectra of Cu HF.

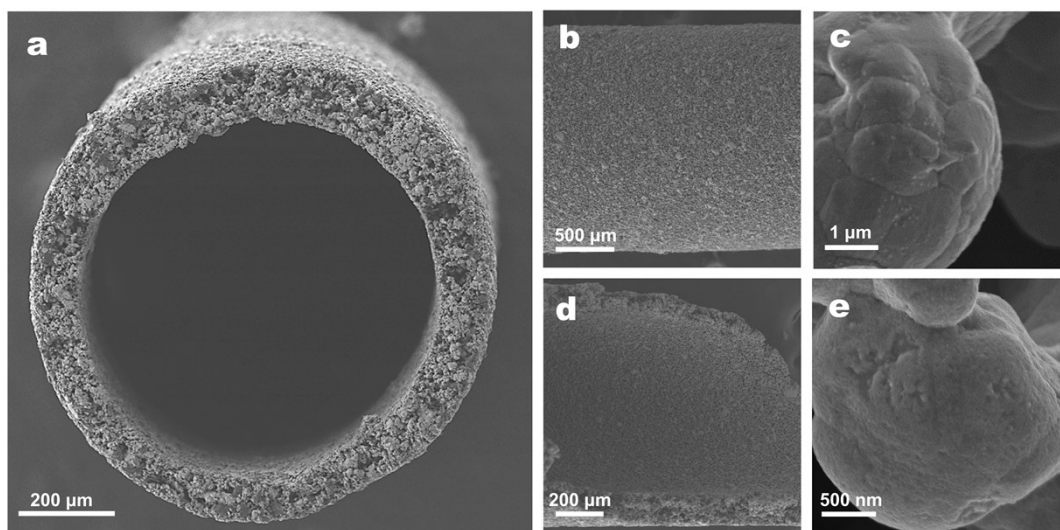


Fig. S2 SEM images of (a) cross-section, (b and c) outer surface and (d and e) inner surface of Cu HF.

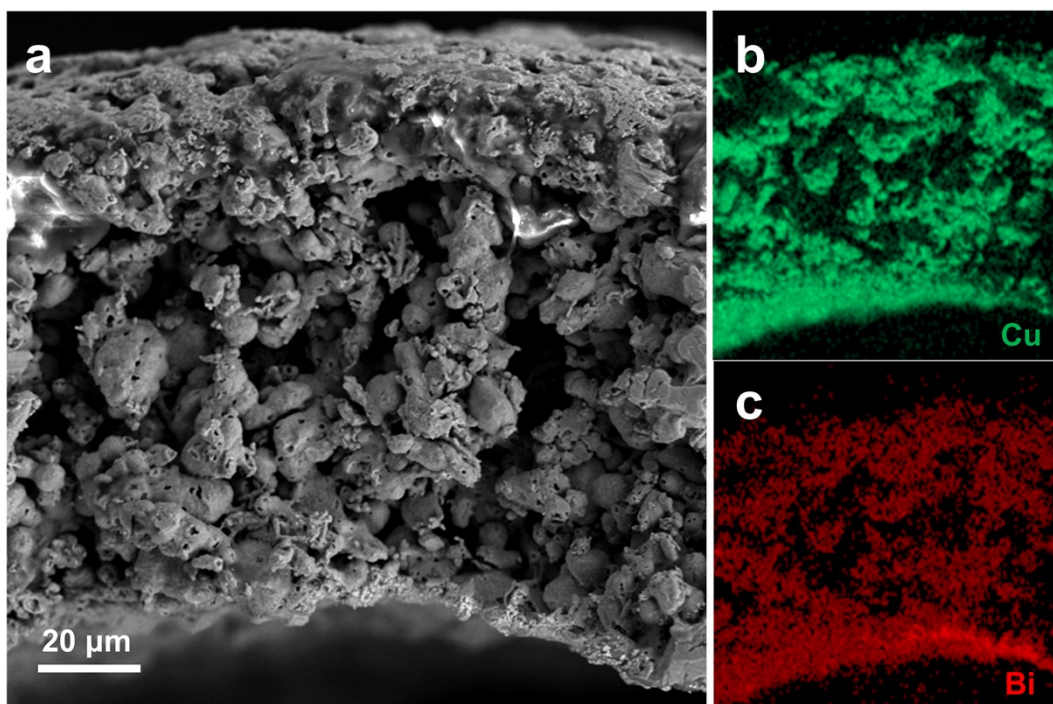


Fig. S3 (a) SEM image of the cross-section of Bi NSAs@Cu HF and (b and c) the corresponding EDX elemental mapping images.

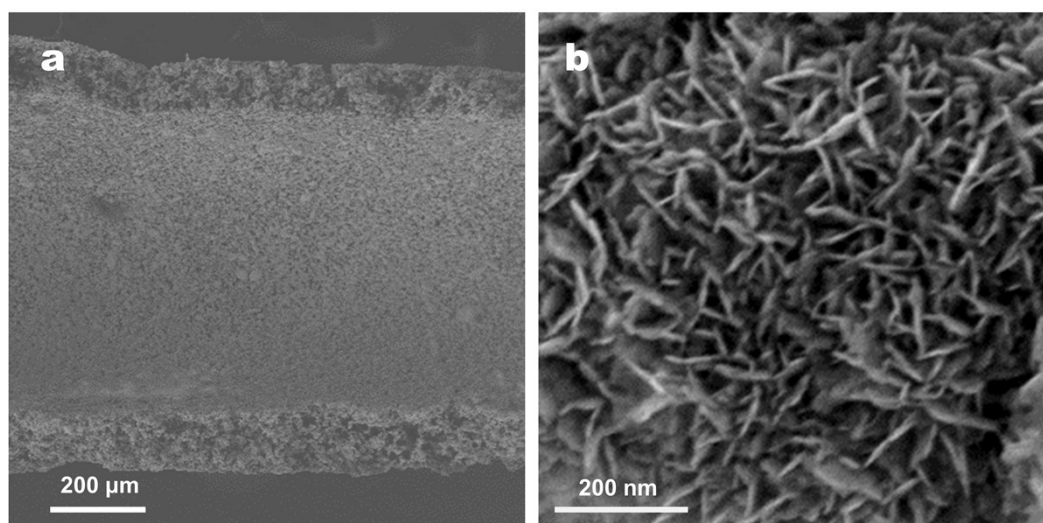


Fig. S4 (a) Low- and (b) high-resolution SEM images of inner surface of Bi NSAs@Cu HF.

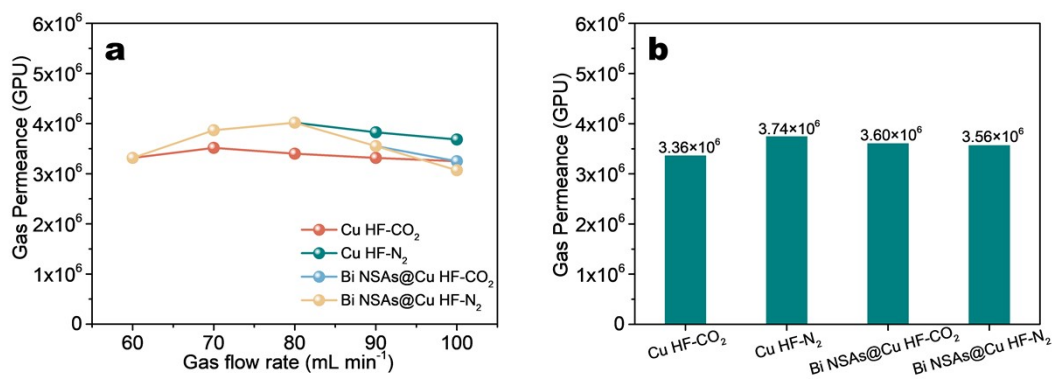


Fig. S5 (a) Gas permeability of Cu HF and Bi NSAs@Cu HF at different gas flow rates. (b) The average gas permeability of Cu HF and Bi NSAs@Cu HF.

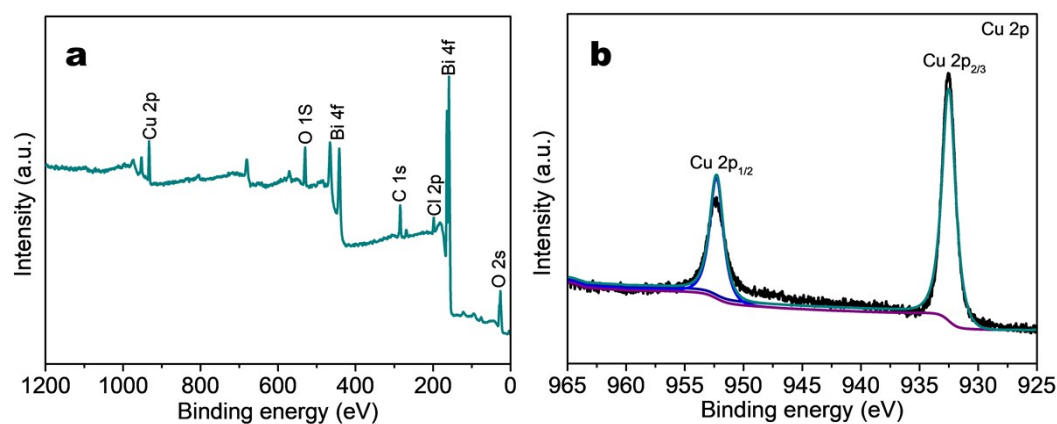


Fig. S6 (a) Survey and (b) Cu 2p XPS spectra of Bi NSAs@Cu HF.

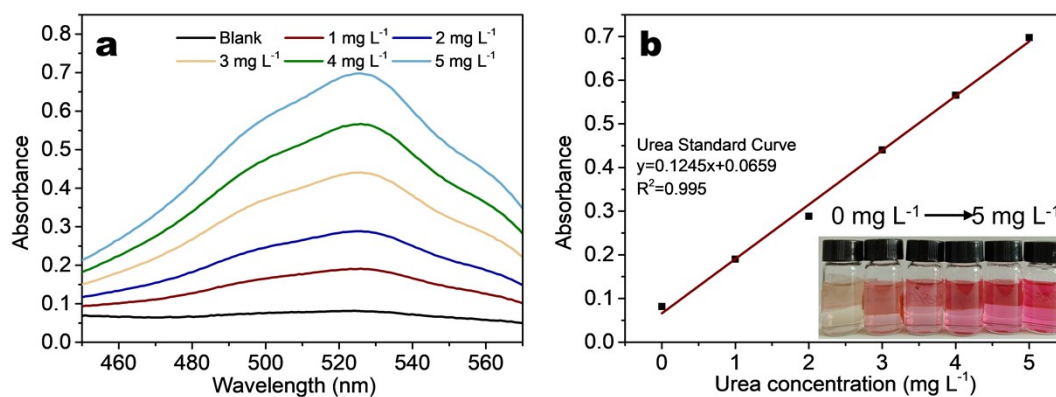


Fig.

S7 (a) UV-vis absorption spectra of urea at different concentrations and (b) the calibration curve used for the determination of urea concentration.

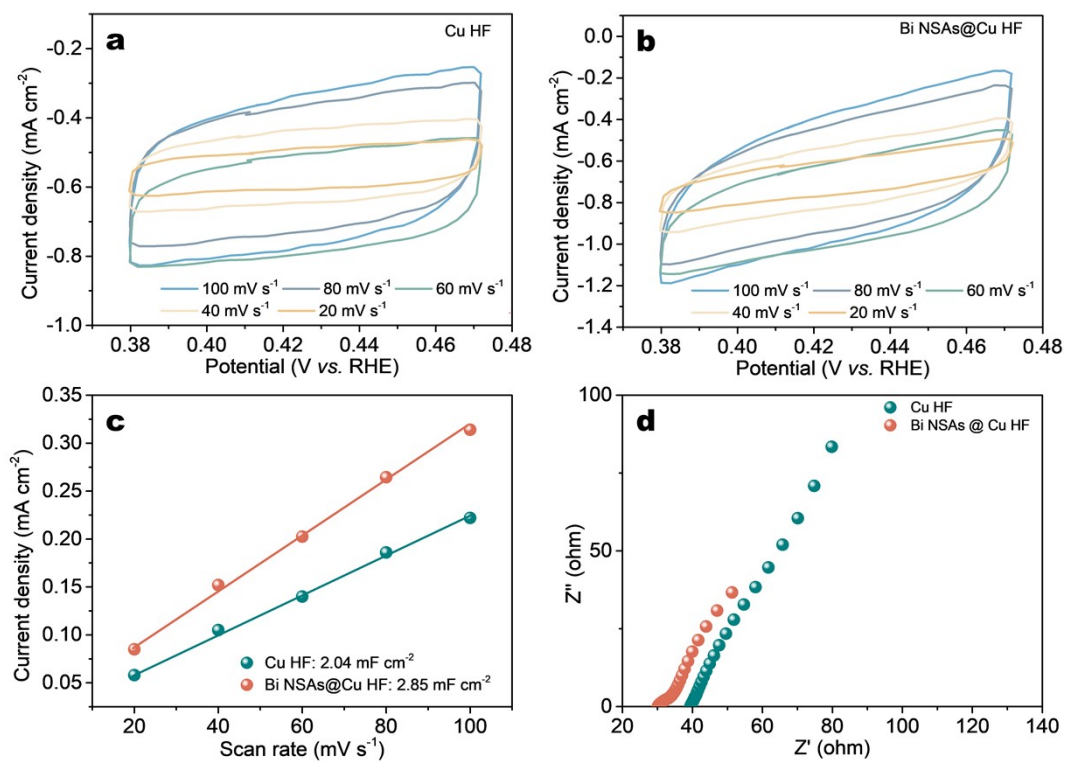


Fig. S8 CV curves of (a) Cu HF and (b) Bi NSAs@Cu HF in the non-Faradaic region at different scan rates. (c) Current density plotted against scan rate for Cu HF and Bi NSAs@Cu HF. (d) EIS curves of Cu HF and Bi NSAs@Cu HF.

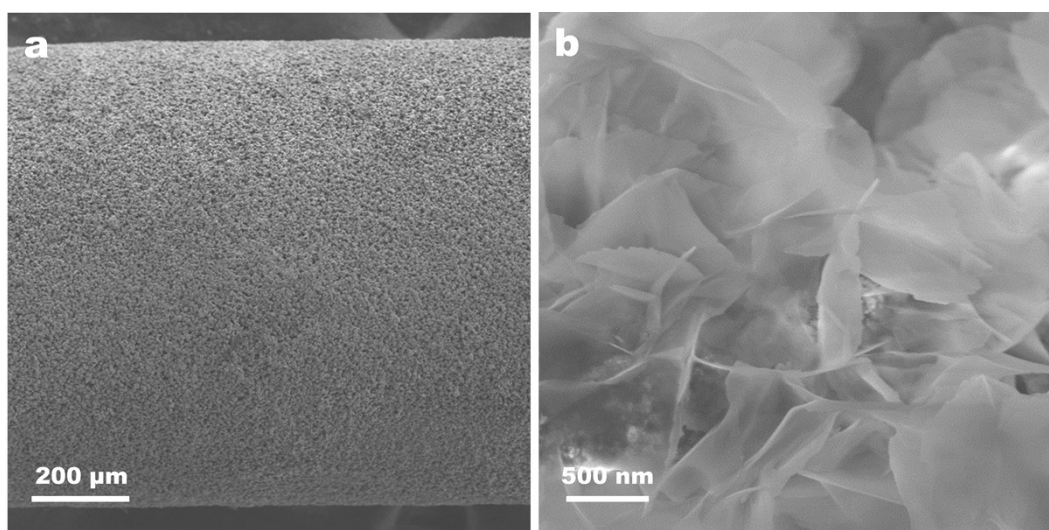


Fig. S9 SEM images of outer surface of Bi NSAs@Cu HF after cycling stability test.

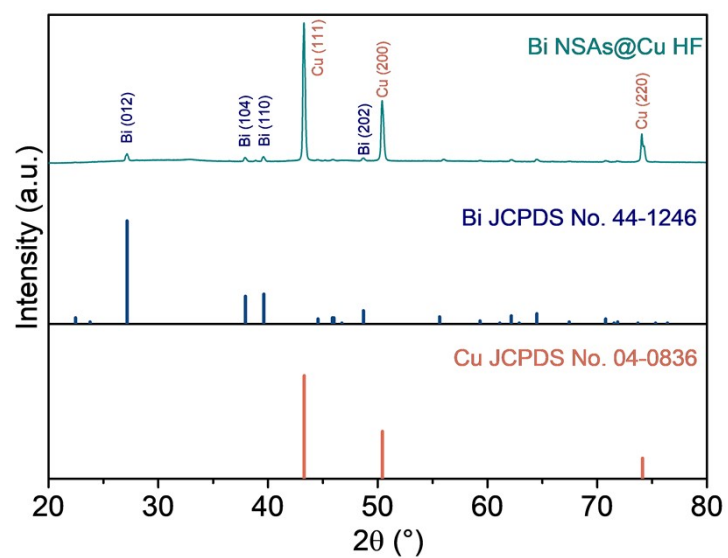


Fig. S10 XRD pattern of Bi NSAs@Cu HF after cycling stability test.

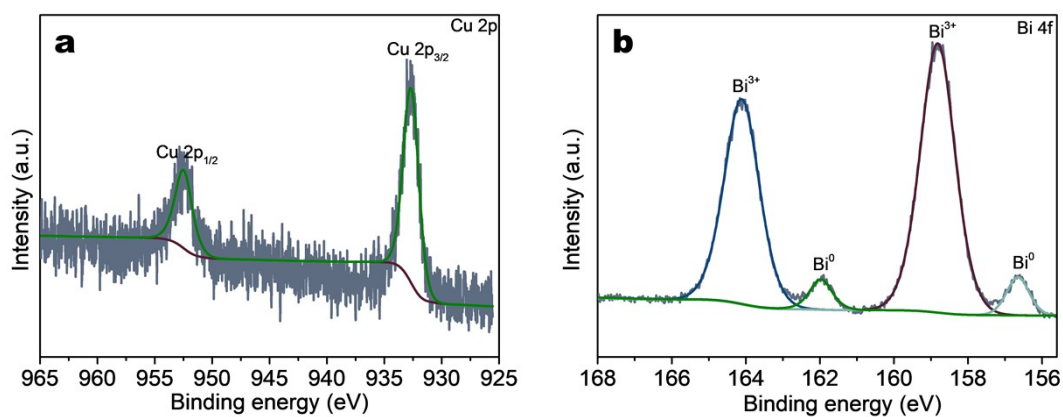


Fig. S11 (a) Cu 2p and (b) Bi 4f XPS spectra of Bi NSAs@Cu HF after cycling stability test.

Table S1. Comparison of the electrocatalytic activity of Bi NSAs@Cu HF with previously reported electrocatalysts for urea electrosynthesis.

Catalysts	Electrolyte	Potential (V vs. RHE)	Urea yield (mmol h ⁻¹ g ⁻¹)	Faradaic efficiency (%)	Ref.
V _N -Cu ₃ N-300	0.1 M KHCO ₃	-0.4	81.0 μg h ⁻¹ cm ⁻²	28.7	5
Pd ₁ Cu ₁ /TiO ₂ -400	0.1 M KHCO ₃	-0.4	3.36	8.92	6
Bi-BiVO ₄	0.1 M KHCO ₃	-0.4	5.91	12.55	7
BiFeO ₃ /BiVO ₄	0.1 M KHCO ₃	-0.4	4.94	17.18	8
Ni ₃ (BO ₃) ₂	0.1 M KHCO ₃	-0.5	9.70	20.36	9
InOOH	0.1 M KHCO ₃	-0.4	6.85	20.97	10
Co-PMDA-2-mnIM	0.1 M KHCO ₃	-0.5	14.5	48.97	11
CuPc NTs	0.1 M KHCO ₃	-0.6	2.39	12.99	12
MoP	0.1 M KHCO ₃	-0.35	0.21	36.5	13
defective Cu-Bi	0.1 M KHCO ₃	-0.4	3.72	8.7	14
ZIF-8	0.5 M KHCO ₃	-0.1	5.45	22.03	15
Ga ₇₉ Cu ₁₁ Mo ₁₀ @C	0.1 M KHCO ₃	-0.4	28.25	60.6	16
Cu-W ₁₈ O ₄₉ @ZIF-8	0.25 M K ₂ SO ₄	-0.9	1.33	8.2	17
Bi ₂ S ₃ /N-RGO	0.1 M KHCO ₃	-0.6	4.4	7.5	18
Bi NSAs@Cu HF	0.1 M KHCO ₃	-0.2	79.0 μg h ⁻¹ cm ⁻²	6.8	This work

Supplementary references

1. C. Zhu, Y. Song, X. Dong, G. Li, A. Chen, W. Chen, G. Wu, S. Li, W. Wei and Y. Sun, *Energy Environ. Sci.*, 2022, **15**, 5391-5404.
2. Z. Meng, F. Wang, Z. Zhang and S. Min, *Nanoscale*, 2024, **16**, 2295-2302.
3. Y. Xia, Z. Meng, Z. Zhang, F. Wang and S. Min, *Energy Fuels*, 2024, **38**, 8062-8071.
4. Rahmatullah, M., and Boyde, T.R.C., *Clin. Chim. Acta.*, 1980, **107**, 3-9.
5. Z. Lv, S. Zhou, L. Zhao, Z. Liu, J. Liu, W. Xu, L. Wang and J. Lai, *Adv. Energy Mater.*, 2023, **13**, 2300946.
6. C. Chen, X. Zhu, X. Wen, Y. Zhou, L. Zhou, H. Li, L. Tao, Q. Li, S. Du, T. Liu, D. Yan, C. Xie, Y. Zou, Y. Wang, R. Chen, J. Huo, Y. Li, J. Cheng, H. Su, X. Zhao, W. Cheng, Q. Liu, H. Lin, J. Luo, J. Chen, M. Dong, K. Cheng, C. Li and S. Wang, *Nat. Chem.*, 2020, **12**, 717-724.

7. M. Yuan, J. Chen, Y. Bai, Z. Liu, J. Zhang, T. Zhao, Q. Wang, S. Li, H. He and G. Zhang, *Angew. Chem., Int. Ed.*, 2021, **60**, 11005-11013.
8. M. Yuan, J. Chen, Y. Bai, Z. Liu, J. Zhang, T. Zhao, Q. Shi, S. Li, X. Wang and G. Zhang, *Chem. Sci.*, 2021, **12**, 6048-6058.
9. M. Yuan, J. Chen, Y. Xu, R. Liu, T. Zhao, J. Zhang, Z. Ren, Z. Liu, C. Streb, H. He, C. Yang, S. Zhang and G. Zhang, *Energy Environ. Sci.*, 2021, **14**, 6605-6615.
10. M. Yuan, H. Zhang, Y. Xu, R. Liu, R. Wang, T. Zhao, J. Zhang, Z. Liu, H. He, C. Yang, S. Zhang and G. Zhang, *Chem Catal.*, 2022, **2**, 309-320.
11. M. Yuan, J. Chen, H. Zhang, Q. Li, L. Zhou, C. Yang, R. Liu, Z. Liu, S. Zhang and G. Zhang, *Energy Environ. Sci.*, 2022, **15**, 2084-2095.
12. J. Mukherjee, S. Paul, A. Adalder, S. Kapse, R. Thapa, S. Mandal, B. Ghorai, S. Sarkar and U. Ghorai, *Adv. Funct. Mater.*, 2022, **32**, 2200882.
13. D. Jiao, Y. Dong, X. Cui, Q. Cai, C. R. Cabrera, J. Zhao, Z. Chen, *J. Mater. Chem. A*, 2023, **11**, 232-240.
14. W. Wu, Y. Yang, Y. Wang, T. Lu, Q. Dong, J. Zhao, J. Niu, Q. Liu, Z. Hao and S. Song, *Chem Catal.*, 2022, **2**, 3225-3238.
15. J. Yuan, Z. Liu, L. Ma, Z. Feng and K. Zhu, *J. Electrochem. Soc.*, 2023, **170**, 043503.
16. Y. Yu, Z. Lv, Z. Liu, Y. Sun, Y. Wei, X. Ji, Y. Li, H. Li, L. Wang and J. Lai, *Angew Chem., Int. Ed.*, 2024, **63**, e202402236.
17. X. Yao, C. Zhu, J. Zhou, K. Zhang, C. Sun, M. Dong, G. Shan, Z. Wu, M. Zhang, X. Wang and Z. Su, *Green Chem.*, 2024, **26**, 8010-8019.
18. P. Xing, S. Wei, Y. Zhang, X. Chen, L. Dai and Y. Wang, *ACS Appl. Mater.*, 2023, **15**, 22101-22111.